

Probing the Sol-Gel Transition in SiO₂ Hydrogels—A New Application of Near-Infrared Fluorescence

Chris D. Geddes,¹ John M. Chevers,¹ and David J. S. Birch¹

Received August 31, 1998; accepted November 19, 1998

Picosecond time-resolved fluorescence spectroscopy has enabled us to use a near-infrared fluorescent dye to probe the sol-gel transition in SiO₂ hydrogels, polymerized from sulfuric acid and sodium silicate solution, for the first time. We compare the microviscosity surrounding the probe during the sol-to-gel transition as predicted by two alternative models which both describe the decay of fluorescence anisotropy well. The results for one rotational time and a residual anisotropy imply that macrogelation of the sol leads to relatively small changes in the mobility of the fluorophore caused by small changes in microviscosity, but after much longer times, e.g., ≈ 1500 min, the mobility of the fluorophore decreases, reflecting a rapid increase in microviscosity of over several orders in magnitude. In sharp contrast, analysis of the anisotropy in terms of two rotational times predicts little change in microviscosity over the whole polymerization process.

KEY WORDS: Sol-gel transition; hydrogels; microviscosity.

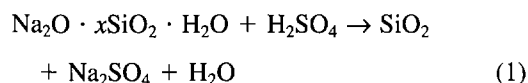
INTRODUCTION

The sol-gel process allows the preparation of room-temperature oxide glasses [1,2]. By utilizing this method it is possible to encapsulate organic dyes in an inorganic matrix at relatively low temperatures, compared to the high temperatures associated with traditional glass-melt technologies [3,4].

Previous fluorescence work has used organic dyes to probe the local chemistry and structure during the sol-to-gel transition in alcogels and metal-silicate composites [5,6]. However, despite having disparate industrial applications which include uses in cleaning agents, liquor refining, and paints, little attention has been given to SiO₂ hydrogels prepared from aqueous sodium silicate (water glass) and sulfuric acid. One explanation for this has been the difficulty of finding suitable fluorescence probes with fluorescence characteristics which are unperturbed by the harsh conditions required for acidic SiO₂ hydrogel synthe-

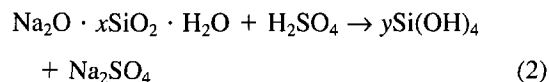
sis. (A typical premixing sulfuric acid concentration ≈ 4.5 mol dm⁻³).

The sol-gel process is a synthetic inorganic polymerization, through a series of hydrolysis and condensation steps of sodium silicate solution. In the simplest case,

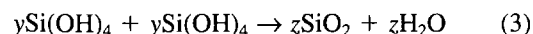


where x represents the mole ratio of the glass.

During the course of the sol-gel process, the first reaction is hydrolysis,



followed by stepwise polymerization by dehydration,



where y and z are integers.

While it can be seen that the hydrolysis is acid catalyzed, it should be noted that the rate is pH dependent. Other parameters such as temperature, pressure, and the

¹ Department of Physics and Applied Physics, University of Strathclyde, John Anderson Building, 107 Rottenrow, Glasgow G4 ONG, UK.

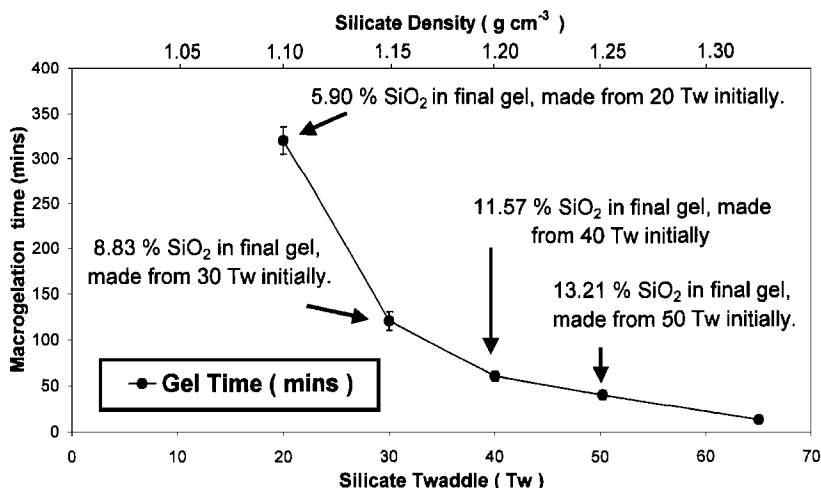


Fig. 1. Macrogelation times for sol-gels made with different initial sodium silicate density (g cm^{-3}) and twaddle (Tw). The density of sulfuric acid was a constant 50.2 Tw (1.251 g cm^{-3}) for all gels, which was titrated by 1 N NaOH at $\approx 4.5 \text{ mol dm}^{-3}$.

concentration of starting materials also affect both the rate and the strength of the final glass.

Because of the ease of preparation and enormous industrial significance, i.e., optical components, fiber drawing, etc., many authors (first reported by Avnir *et al.* [7]), have encapsulated organic molecules in alcogels and strived to understand the changes in a probe's response during the sol-to-gel transition. For example, the local microviscosity of rhodamine 6G encapsulated in a tetramethyl orthosilicate (TMOS) gel has recently been reported [8].

In this paper we report a fluorescent probe's response to viscosity changes, in the sol-to-gel transition for hydrogels. A xanthene-type dye (JA120) is introduced into glass solutions prior to gelation and both the fluorescence anisotropy and the lifetime are recorded as a function of time. Data acquisition times of a few minutes were insignificant in comparison to the gelation times. While the initial acid concentration remained constant [4.5 mol dm^{-3} , 50.2 twaddle (Tw),² 1.251 SG, 34%], the silicate densities used were 20, 30, 40, and 50 Tw. This produced final gels with 5.90, 8.83, 11.57, and 13.21% SiO₂ with macrogelation times (MGT) of 5.5 h, 2 h, 60 min, and 40 min, respectively, as shown in Fig. 1.

THEORY

The theory of time-resolved fluorescence anisotropy has been reviewed many times [9,10]. A few of the key expressions used in this paper are highlighted.

² The twaddle (Tw) is a unit of density first used at the turn of the century, to enable workers to deal easily with integers. The twaddle is frequently used as an industrial unit. SI conversion: twaddle = 200 (density/ $\text{g cm}^{-3} - 1$).

Using vertically polarized excitation, the intensity of fluorescence at parallel (F_p) and crossed (F_x) emission polarizer orientations will depend on the rotation of the fluorophore in the excited state. The time-dependent depolarization of fluorescence can be expressed by the anisotropy function $R(t)$:

$$R(t) = \frac{F_p(t) - F_x(t)}{F_p(t) + 2F_x(t)} \quad (4)$$

From the Perrin expression rotational information can be gained as one obtains a direct relationship between $R(t)$ and the rotational correlation time τ_R of an unbound fluorophore.

$$R(t) = R_0 e^{-t/\tau_R} \quad (5)$$

where R_0 is the initial anisotropy at time 0 and which has a maximum value of 0.4. In terms of the simple Stokes-Einstein theory, τ_R is related to the microviscosity (η) encountered by the fluorophore:

$$\tau_R = \eta V / kT \quad (6)$$

where η is the viscosity of the medium (poise), V the molecular volume, k the Boltzmann constant, and T the absolute temperature.

In the case of hindered molecular rotation, such as for a fluorophore bound to a macromolecule, which rotates on a much longer time scale than the fluorescence lifetime, or in an ordered medium such as a lipid bilayer membrane in the gel phase, the fluorescence is only partially depolarized, leading to a residual anisotropy function, R_∞ , given by

$$R(t) = (R_0 - R_\infty) \exp(-t/\tau_r) + R_\infty \quad (7)$$

In this case τ_r reflects the vicinal viscosity close to the

binding site, which may be markedly different from that in bulk solution described by Eq. (6).

It is widely recognized that the statistical precision of anisotropy data is rarely capable of supporting an interpretation more complex than two rotational times. Indeed a fluorescence ambiguity occurs in many heterogeneous systems in terms of distinguishing between Eq. (7) and a two-rotational time model representing dual environments for the probe given by

$$R(t) = (1 - f) R_0 \exp(-t/\tau_{r1}) + fR_0 \exp(-t/\tau_{r2}) \quad (8)$$

where fractions f and $1 - f$ of the total fluorescence can be attributed to probe molecules in two environments with two distinct rotational times. It is particularly difficult telling the difference between Eq. (7) and Eq. (8) in cases such as we have here, where the fluorescence lifetime of the dye (≈ 2.5 ns initially in the sol gels studied) is much shorter than the time scale of depolarization.

EXPERIMENTAL

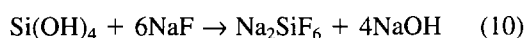
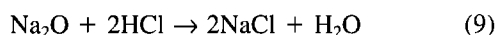
Materials

The 79.5-Tw sodium silicate solution (Crystal 79) and 50% sulfuric acid were supplied by Crosfield Chemicals Ltd.; 20- to 50-Tw sodium silicate solutions were made by dilution of Crystal 79 with doubly distilled deionized water. The 1 *N* NaOH, 1 *N* HCl, and 0.2 *N* HCl volumetric standards were purchased from Aldrich Chemical Co. Ltd. Methyl Red and Universal indicator solutions were purchased from Fisons. The fluorescent dye (JA120)[11] was kindly supplied to us by Dr. J. Arden-Jacob, University of Seigen, Germany.

Solution Preparation

The concentration of 50.2-Tw, 34% sulfuric acid was a constant 4.5 mol dm⁻³ as determined by titration with 1 *N* NaOH solution.

The % Na₂O in sodium silicate (Na₂O · xSiO₂ · yH₂O) was determined by titration with HCl (Eq. 9); while the % SiO₂ was determined by titrating the NaOH liberated from the reaction of Si(OH)₄ with NaF [Eq. (10)] with HCl.



Sol-Gel Preparation

This procedure outlines the typical production of an 18% SiO₂:5.5% Na₂SO₄ final gel, made from 65-Tw

sodium silicate solution and 50.2-Tw 34% (≈ 4.5 mol dm⁻³) sulfuric acid. The physical characteristics and gelation times of the final gel can be altered by using different starting compositions. Solutions of silicate and acid were delivered separately to a mixing head using peristaltic pumps. The mixing head was of stainless-steel construction incorporating mixing blades rotating at 1200 rpm in order to ensure a homogeneous sol mixture and hence prevent localized gelation. The 50.2-Tw sulfuric acid is pumped at ≈ 2.78 mls⁻¹ into the 300-ml mixing head. After 30 s (the volume run is 83.5 ml), 65-Tw (7% Na₂O:26% SiO₂) sodium silicate is pumped into the head at ≈ 6.75 mls⁻¹. Final sol-gel solutions are collected after 135 s; the solution collected prior to 135 s was run to waste. The macrogelation time (MGT; the time for the solution, Sol., to set firm) was 11.5–13.5 min, as shown in Fig. 1.

The JA120 fluorophore was added to the bulk mix immediately after mixing and cast into 3-cm³ unsealed plastic cuvettes (Hughes & Hughes Ltd). The cuvettes were weighed on a Mettler AJ50 top pan balance in parallel with anisotropy measurements to determine the weight loss of water, by evaporation, as a function of time.

Excess Sol-Gel Normality

The excess sulfuric acid normality of the final gels was taken prior to solution gelation and was determined by acid–base titration with 1 *N* NaOH. Gels with short gelation times were diluted with doubly distilled deionized water, prior to gelation, to prevent auto gelation. The excess sulfuric acid normality for 20- to 50-Tw, 5.90→13.21% SiO₂ gels was found to be 1.91, 1.63, 1.14, and 0.77 *N*, respectively.

Probe Volume Determination

Time-resolved anisotropy, measured at 20°C, for JA120 in a range of solvents, enabled the probe molar volume to be determined using Eqs. (4)–(6) (Table I).

Table I. Probe Radius Calculation Data

Solvent	$\tau_r(\text{ps})^a$	η (cP) ^b	Probe radius (Å)
H ₂ O	316	1.002	3.123
Ethanol	535	1.200	3.505
Propan-1-ol	1050	2.256	3.556
Butan-1-ol	1370	2.948	3.554

^a Probe rotational time.

^b Viscosity of solvent.

From these data we calculated the JA120 radius. A mean radius of 3.5 Å was subsequently used to follow the microviscosity of the four sol-gel systems studied. Considering the structure of JA120 [11], one could, assuming a typical carbon-carbon bond length of 1.2 Å, estimate the radius to be ≈ 7 Å. Smaller probe radii are commonly calculated for a “slipping rotor” system, a system where no solvent is displaced during molecular rotation and hence the rotational friction coefficient is zero. In systems where a “stick” model is used, then solvent molecules are “dragged” during molecular rotation and hence probe radii are commonly overestimated. In reality molecules are thought to experience a combination of “slip” and “stick” boundary conditions [12], but such models are complicated and beyond the scope and application of the present work. Whilst the calculated probe radii may differ slightly, due to the chosen model, the viscosity trends remain the same.

Fluorescence Measurements

All steady-state fluorescence measurements were performed on a Perkin Elmer luminescence spectrometer, LS 50B, with 2-nm slits for excitation and emission. Excitation spectra are corrected with respect to the lamp spectral profile. Emission spectra are uncorrected for the instrumental spectral response.

Fluorescence decay kinetics were studied using the TCSPC technique. A Hamamatsu PLP-02 diode laser with a 650-nm laser head and giving a ≈ 50 -ps pulse was used for vertically polarized excitation. Emission was collected at >720 nm, using a Kodak

cutoff filter, and dichroic sheet polarizers (Halbo Optics) were toggled between vertical and horizontal orientations to obtain the anisotropy data. A single-photon avalanche photodiode, CD2027 (supplied by EG & G), was the detector. All measurements were taken at 20°C.

RESULTS AND DISCUSSION

The absorption spectrum for JA120 in 50% (sp grav, 1.40) sulfuric acid, with respect to that in water (Fig. 2) shows an ≈ 5 -nm bathochromic shift in absorption maxima. This reflects the slightly more polar acidic medium. Absorption spectra during the sol-to-gel transition over the time periods discussed in this paper showed no significant changes.

The emission spectrum for JA120 in water at 20°C (Fig. 3) indicates one ground-state species with peak $\lambda_{em} = 690$ nm. To reproduce the thermal effects encountered by the dye, due to the acid-base heat of neutralisation (i.e., the mixing of sulfuric acid and sodium silicate solution), both absorption and emission spectra were taken as a function of temperature, 10–40°C. These temperature increases had no significant effect on the fluorescence characteristics. Further evidence for the stability of the dye could be found in the fluorescence lifetime data whereby the lifetime is seen in Fig. 4 to increase gradually with gelation from an initial value of ≈ 2.5 ns. A weak decay component of ≈ 1.5 ns with a few percent of the total emission, which might be a dye impurity, was also observed to

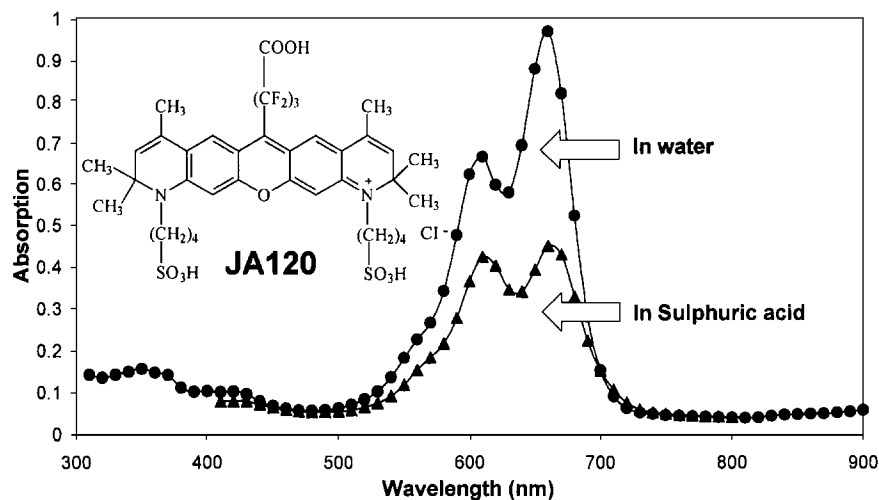


Fig. 2. Absorption spectra for JA120 in both deionized water and 50% sulfuric acid and the molecular structure of JA120. Cl^- , counter ion.

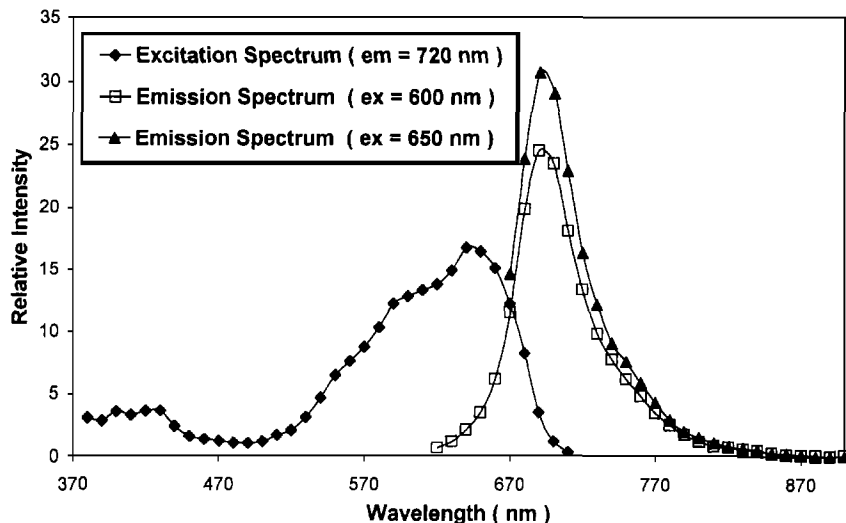


Fig. 3. Excitation and emission spectra for JA120 in deionized water at 20°C.

increase gradually, but this was, in any case, taken account of in the anisotropy impulse reconvolution.

Data analysis was performed using nonlinear least squares with the IBH iterative reconvolution library.

Analysis of the anisotropy data for 20- to 50-Tw sol-gels showed comparable goodness of fit when fitted to one rotational time and a residual anisotropy [Eq. (7)] and two rotational times [Eq. (8)]. Viscosities calculated using one rotational time with the former model are shown in Fig. 5 and the trend shown is typical of all the sol-gels studied. Namely, the microviscosity of the sols remains reasonably constant,

before and after the respective macrogelation times, before drastically increasing well after the macroscopic gel point has been reached. This behavior, which at first might seem surprising, suggests that the probe exists in a wholly fluid environment, even after the gelation point. Figure 6 shows that water is lost by syneresis and subsequent evaporation as the porous gel network formed at the gelation point begins to shrink [1]. Since the dye is cationic, it is likely to bind to silica, and in this case the viscosity might reflect that of vicinal water trapped within pores and interconnecting channels. In contrast, a model describing the anisotropy

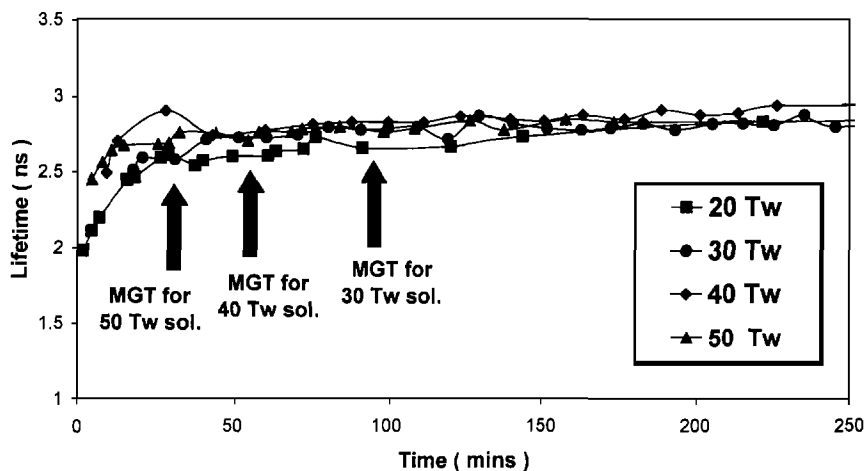


Fig. 4. Fluorescence lifetime of JA120 as gelation proceeds in different sols. MGT, macrogelation time.

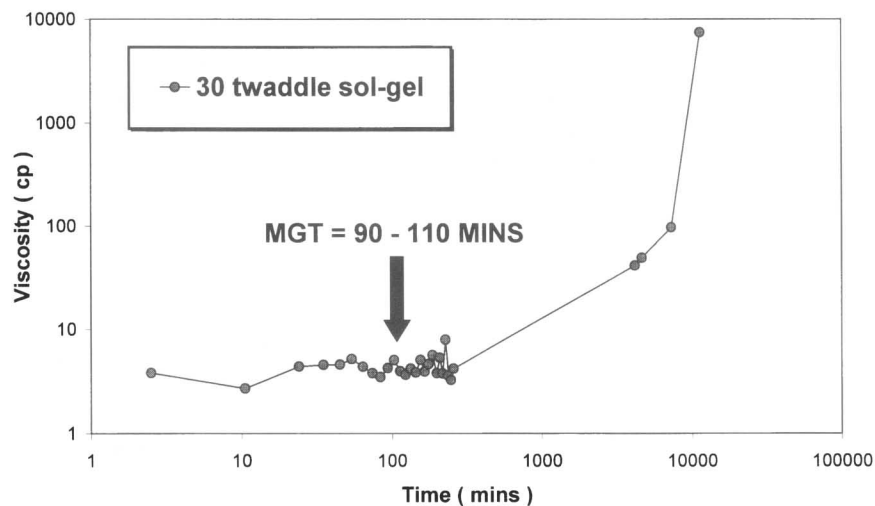


Fig. 5. Microviscosity for a 30-Tw, 8.83% final SiO_2 sol-gel, assuming a one-rotational time decay of fluorescence anisotropy. All sol-gels showed an increase in microviscosity after ≈ 1500 min. MGT, macrogelation time.

decay in terms of two rotational correlation times shows little change in the microviscosity sensed by the dye for all the sol-gels, not only initially, but over the whole polymerization process, and this is illustrated in Fig. 7. Again, this implies that the dye always senses a fluid environment, but in this case the implication is that the fluid present is dominated by that of the bulk solution even after gelation. A surprising feature

of both models is that the probe does not sense the point of macrogelation, and this must reflect the probe's preference for taking up an aqueous rather than a silicate environment. The second rotational time increases with gelation to levels approaching 100 ns and a major factor in interpreting this is whether or not such long rotational times can be measured with a 2.5-ns fluorescence lifetime.

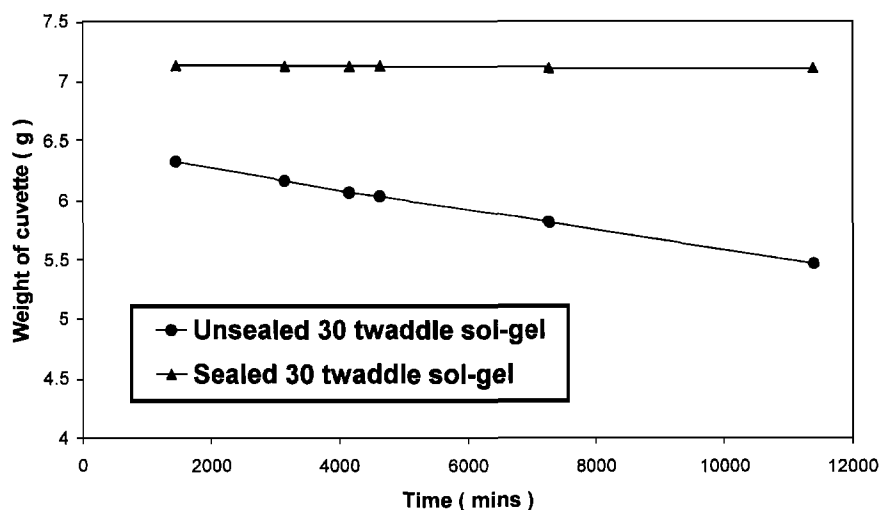


Fig. 6. Weight loss for a 30-Tw sol-gel. One sample was sealed initially. The weight loss by the unsealed sample is indicative of water loss by evaporation, post gel syneresis. Note also that both cuvettes contained different quantities of sol-gel and hence do not extrapolate to the same point at time = 0 min. The unsealed sample was used for all 30-Tw time-resolved fluorescence measurements.

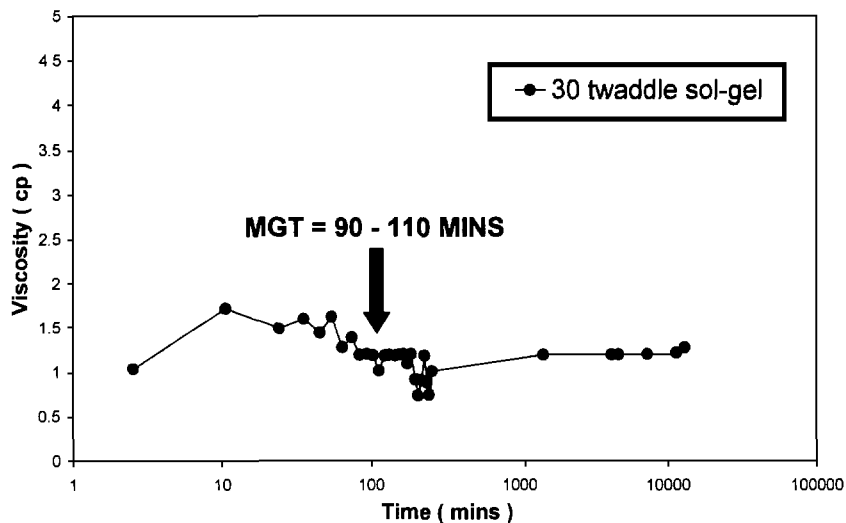


Fig. 7. Microviscosity for a 30-Tw, 8.83% final SiO₂ sol-gel, assuming a two-rotational time decay of fluorescence anisotropy. MGT, macrogelation time.

CONCLUSIONS

In this paper we have shown how a near-infrared fluorophore can probe and provide useful information during the sol-to-gel transition in hydrogels. In particular, we have demonstrated that microscopic changes reported by the dye do not coincide with the bulk changes incurred at the gelation point.

Further work is presently under way to distinguish between the two quite opposite interpretations of the anisotropy decay, described by either a second rotational time or a residual anisotropy, by producing sol-gels where either the acid normality or the silicate concentration is kept constant. This will simplify the interpretation and, at the same time, produce a number of anisotropy curves from which small differences in the goodness of fit, which are not meaningful in a single measurement, might become significant when the wider picture is taken into account. Further progress, to bridge our understanding of the relationship between micro- and macroscopic properties of silica hydrogels, hinges on being able to make such a distinction. Our results of this further investigation will be reported shortly.

ACKNOWLEDGMENTS

We would like to thank the EPSRC and Unilever for financial support. We would also like to thank Dave Ward, Unilever, for informative discussions.

REFERENCES

1. C. J. Brinker and G. Scherer (1989) *Sol-Gel Science, The Physics and Chemistry of Sol-Gel Processing*, Academic Press, San Diego.
2. L. L. Hench and J. K. West (1990) *Chem. Rev.* **90**, 33.
3. P. B. Hunt and J. L. R. Noguez (1995) *Laser Focus World* **31**(12), 90.
4. D. R. Ulrich (1988). *Chemtech.* **18**(4), 242.
5. T. Fujii, H. Kitamura, O. Kawauchi, T. Mabuchi, and N. Negishi (1991) *J. Photochem. Photobiol. A Chem.* **61**, 365.
6. B. Dunn and J. I. Zink (1991) *J. Mater. Chem.* **1**(6), 903.
7. D. Avnir, D. Levy, and R. Reisfeld (1984) *J. Phys. Chem.* **88**, 5956.
8. F. V. Bright, U. Narang, R. Wang, and P. N. Prasad (1994) *J. Phys. Chem.* **98**, 17.
9. J. R. Lakowicz (1983) *Principles of Fluorescence Spectroscopy*, Plenum Press, New York.
10. D. J. S. Birch and R. E. Imhof (1991) *Topics in Fluorescence Spectroscopy, Vol. 1. Techniques*, Plenum Press, New York, pp. 1–95.
11. K. H. Drexhage, N. J. Marx, and J. Arden-Jacob (1997) *J. Fluoresc.* **7**(1) 91s.
12. C. Hu and R. Zwanzig (1974) *J. Chem. Phys.* **60**(11), 4354.